Theor Chim Acta (1987) 71: 425–448

Theoretica Chimica Acta

Investigations with the finite element method on the Cyber 205

I. The collinear X + YZ (X, Y, Z = H, D, Mu) reaction

Ralph Jaquet

Theoretische Chemie, Universität Siegen, D-5900 Siegen, Federal Republic of Germany

(Received January 27, revised and accepted February 10, 1987)

We are trying to investigate systematically the application of the finite element method (FEM) for solving the Schrödinger equation. The present paper is devoted to the calculation of vibrational transition probabilities for the collinear reactive system A + BC (i.e. $H + H_2$ and their isotopes). The calculations are fully two-dimensional and the results are compared with earlier FEM calculations and conventional basis set expansion methods using the the *R*-matrix or *S*-matrix propagation.

We made extensive analysis of FEM on the vector-computer Cyber 205 and developed a vector code for the efficient use in two dimensions, so that in the near future applications even in three dimensions will be possible.

For the hydrogen exchange reactions we investigated the following isotope combinations: (a) $H + H_2$, b) H + DH, D + HD and H + MuH (symmetric reaction), (c) D + HH, H + DD and Mu + DD (asymmetric reaction). We calculated the transition probabilities for up to five open vibrational channels and found excellent agreement with known "exact" values.

Key words: Finite element method — Collinear hydrogen isotope reaction — Vibrational reaction probabilities

1. Introduction

Since the last ten years there has been a rapid development in computer technology, especially an increase of core memory and computing power [1]. Supercomputers are well designed to matrix algebra and therefore fit to the need of

quantum chemistry. The solution of the Schrödinger-equation for electronic structure calculations and for the dynamics of atomic and molecular motion is nowadays well established by basis set expansion methods [2], which very often cannot optimally use the computer architecture [3]. For example, a disadvantage of the supercomputer Cyber 205 is that the optimum speed can be reached only for a vector length N in the matrix algebra greater than 200 [1, 3].

The special features of supercomputers led us to expect that the finite element method (FEM) might be a useful tool for solving the Schrödinger equation in few dimensions. Although one has to work with very large matrix systems ($N = 1000$–$100\,000$) an efficient solution can be reached in case of a large core memory. Our code for FEM has been adapted to a Cyber 205.

The aim of this paper was to use FEM for the investigation of dynamical problems, especially the reactive scattering dynamics between atoms and diatomic molecules. There has been significant progress in treating molecular collisions theoretically [4], but many difficulties still remain to be solved, especially for the exact solution of scattering in more than two dimensions.

In the past three decades the development of numerical FEM procedures for solving differential equations has reached a very high level [5]. In continuum mechanics FEM has already replaced conventional methods like finite difference and variational methods. The use of FEM in different fields of classical mechanics is increasing. A similarity between finite difference and finite element methods relates to the discretization of the integration area by grid points or into so called elements, respectively. There is substantial advantage in FEM, because of flexibility of choosing irregular meshes, treatment of special boundary conditions, and optimizing the local wavefunctions inside each element.

First investigations with FEM for solving the Schrödinger equation started about ten years ago: (a) the eigenvalue problem of the H-atom in one dimension [6], (b) the vibrational problem of diatomic molecules [7] and (c) the H-atom treated in two dimensions [8]. Askar, Cakmak and Rabitz [9] showed how to use FEM for reactive scattering and calculated the vibrational transition probabilities for $v = 0$ and 1 for the collinear reaction of $H + H_2$. The same authors use FEM for different two-dimensional eigenvalue problems [9c]. In the following years a few scattering investigations using FEM have been performed [10].

In the last four years FEM gained more and more popularity. Linderberg et al. [11] and Kuppermann and Hipes [12] are using this method for solving the three-dimensional reactive scattering dynamics of $H + H_2$ and $F + H_2$ by propagating the eigenfunctions in the two hyperspherical angle coordinates. In the case of electron-hydrogen collision Christensen-Dalsgaard [13] made considerable progress and Levin and Shertzer [14] calculated the eigenvalue problem for the Helium ground state in three dimensions. Askar and Rabitz [15] have performed the first full 3D rotational inelastic scattering calculation for $H + H_2$. Within the concept of finite elements there are many possibilities of defining local basis functions. Normally one uses quadratic or cubic polynomials, but Schulze and Kolb [16] showed in their two-dimensional calculations for the eigenvalues of

H_2^+ that quintic polynomials are very efficient and reduce the size of the matrix problem considerably.

In this series of papers we want to investigate systematically how to use FEM for solving the Schrödinger equation. This first paper will be devoted to the calculation of vibrational transition probabilities for the reactive system A+BC (i.e. $H+H_2$ and their isotopes in collinear geometry).

Although the theory of FEM is written up in many textbooks [5], a short overview will be given. For more detailed information the reader may be referred to the work of Linderberg [11c] or the paper of Askar et al. [9].

The adaption of FEM to the special capability of the Cyber 205 is described in Chap. 4, and in Chap. 5 some examples of our calculations for the hydrogen isotope reactions will be shown. In further papers we will explain our calculations for special systems in more detail.

2. Formalism

2.1. General outline

In the following we will be concerned with mathematical two-dimensional partial differential equations. For the time-independent Schrödinger equation

$$(H-E)\varphi = 0 \tag{1}$$

on domain G we use a variational condition which is equivalent to a functional equation

$$\delta L = \int_G \delta\varphi (H-E)\varphi \, \mathrm{d}G = 0. \tag{2}$$

For the two-dimensional case with potential $V(x, y)$ and reduced mass μ, partial integration and the Gauss theorem yields:

$$\delta L = \int_G \left[\frac{\hbar^2}{2\mu} \nabla\delta\varphi\nabla\varphi + \delta\varphi(V-E)\varphi \right] \mathrm{d}G - \frac{\hbar^2}{2\mu} \oint_C \delta\varphi \frac{\partial\varphi}{\partial n} \mathrm{d}s = 0. \tag{3}$$

The second part is a line integral over the closed boundary (Dirichlet condition) with $\delta\varphi = 0$, resulting in:

$$\delta L = \int_G \left[\frac{\hbar^2}{2\mu} \nabla\delta\varphi\nabla\varphi + \delta\varphi(V-E)\varphi \right] \mathrm{d}G = 0. \tag{4}$$

The solution of this equation is a stationary solution for a given boundary condition. In order to solve the scattering problem one has to solve (4) with different choices of boundary conditions; the number of independent different boundary conditions corresponds to the number of channels.

The general idea of FEM is now the following [5b]:
(a) The domain G is discretized in many subdomains called elements. This can be done in many different ways, so that the form of the elements can be fitted

optimally to the problem. In two dimensions triangles or quadrilaterals with straight or curvilinear boundaries can be used. This kind of discretization can be very flexible, but in order to avoid numerical problems, the angles of the elements must not be too small.

(b) On each element the wavefunction φ is approximated by parametrized functions u. We introduce a local approximation of the wavefunction which may be optimally adapted to the problem. The simplest choice are polynomials of different degrees

$$u(x, y) = \sum_{i,j} c_{ij} x^i y^j. \tag{5}$$

At the boundary of two elements the function have to fulfill continuity and differentiability conditions which depend on the problem. Conforming elements are those which fulfill the continuity condition. For further details see [5b].

(c) In each element a certain number of grid points, the so called nodes or knots, are chosen and the functions u in the element e is expanded as

$$u^{(e)}(x, y) = \sum_{i=1}^{p} u_i^{(e)} N_i^{(e)}(x, y); \qquad u_i^{(e)} = u(x_i, y_i), \tag{6}$$

where the "basis" consists of formfunctions $N_i^{(e)}$ which have to be suitably chosen with the properties

$$N_i^{(e)}(x_j, y_j)) = \begin{cases} 1 & \text{for } j = i \\ 0 & \text{for } j \neq i. \end{cases} \tag{7}$$

By this procedure the unknown variables to be determined are the $u_i^{(e)}$, i.e. the values of the functions u at the knots, (and in some formulations also the partial derivatives) instead of the coefficients c_{ij} of (5).

(d) The integral in Eq. 4 has to be taken over the whole domain G and is a sum over all elements

$$\delta L = \sum_e \delta L_e \tag{8}$$

where δL_e is the integral over the element e with area G_e.

2.2. Two-dimensional elements

At present it is not yet clear which form of 2D-elements is the best for our problems. In the following we will describe how the integrals for Eq. 4 have to be calculated in case of triangular elements with six knots using quadratic polynomial functions. In order to get a simple integration formula, we define a linear coordinate transformation from any triangle to an isoceles rectangular unit triangle T_1 (see Fig. 1)

$$\begin{aligned} x &= x_1 + (x_2 - x_1)\xi + (x_3 - x_1)\eta \\ y &= y_1 + (y_2 - y_1)\xi + (y_3 - y_1)\eta \end{aligned} \tag{9}$$

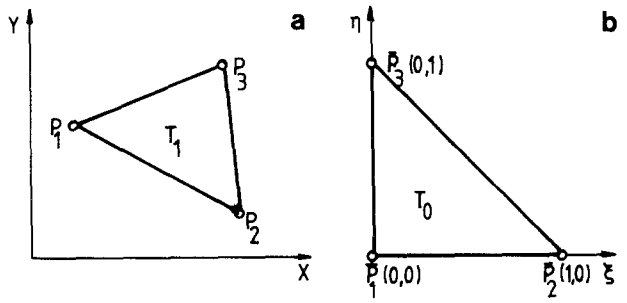

Fig. 1. a General triangle T_1; b unit triangle T_0 with points $\bar{P}_i(\xi, \eta)$

Because of the transformation the calculation of integrals for T_1 is now changed to a "simple area integral" for T_0. The area element is

$$dx\, dy = J\, d\xi\, d\eta, \tag{10}$$

where the Jacobi determinant J is given by

$$J = \begin{vmatrix} \frac{\partial x}{\partial \xi} & \frac{\partial y}{\partial \xi} \\ \frac{\partial x}{\partial \eta} & \frac{\partial y}{\partial \eta} \end{vmatrix} = (x_2 - x_1)(y_3 - y_1) - (x_3 - x_1)(y_2 - y_1) = 2G_e. \tag{11}$$

Partial derivatives of the function u can be expressed by means of the chain rule as

$$\begin{aligned} u_x &= u_\xi \xi_x + u_\eta \eta_x \\ u_y &= u_\xi \xi_y + u_\eta \eta_y \end{aligned} \tag{12}$$

with

$$\begin{aligned} \xi_x &= \frac{y_3 - y_1}{J}, & \eta_x &= -\frac{y_2 - y_1}{J} \\ \xi_y &= -\frac{x_3 - x_1}{J}, & \eta_y &= \frac{x_2 - x_1}{J}. \end{aligned} \tag{13}$$

For the numerical work with formfunctions and for formal illustration it's also useful to use "natural triangle coordinates" ζ_i, which are defined by (Fig. 2).

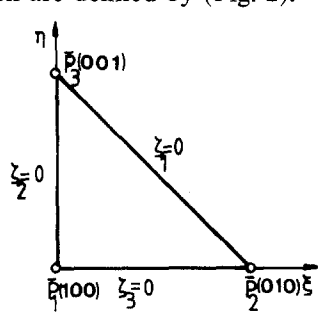

Fig. 2. Natural coordinates in unit triangle with points $\bar{P}_i$ $(\zeta_1, \zeta_2, \zeta_3)$

$$\begin{aligned}\zeta_1 &= 1-\xi-\eta \\ \zeta_2 &= \xi; \qquad \zeta_1+\zeta_2+\zeta_3 = 1. \\ \zeta_3 &= \eta\end{aligned} \tag{14}$$

In case of a quadratic function the coordinates ζ_i of the six knots are given by:

$$\begin{aligned}&P_1(1,0,0);\ P_2(0,1,0);\ P_3(0,0,1); \\ &P_4(\tfrac{1}{2},\tfrac{1}{2},0);\ P_5(0,\tfrac{1}{2},\tfrac{1}{2},);\ P_6(\tfrac{1}{2},0,\tfrac{1}{2},).\end{aligned} \tag{15}$$

All integrals in Eq. 4 are of the general form

$$\int_{G_e} f\,\mathrm{d}G_e = 2G_e \int_0^1 \int_0^{1-\zeta_2} f(\zeta_1,\zeta_2,\zeta_3)\,\mathrm{d}\zeta_1\,\mathrm{d}\zeta_2. \tag{16}$$

Since the function $u(x, y)$ are polynomials all integrals are polynomials. This also holds for the potential energy (i.e. if the potential energy is expressed by polynomials). The general formula of these integrals [5b] reads

$$\int_{G_e} \zeta_1^i \zeta_2^j \zeta_3^k\,\mathrm{d}G_e = \frac{i!j!k!}{(i+j+k+2)!}\,2G_e. \tag{17}$$

The quadratic function $u^{(e)}(x, y)$ (Eq. (6)) is expressed by the values u_1^e (e = element, 1 = number of knot)

$$u^{(e)}(x,y) = u^{(e)}(\zeta_1,\zeta_2,\zeta_3) = \sum_{l=1}^{6} u_l^{(e)} N_l(\zeta_1,\zeta_2,\zeta_3). \tag{18}$$

The formfunctions as used in Eq. (6) may be expressed in terms of ζ_i [5b]:

$$\begin{aligned}N_1(\zeta_1,\zeta_2,\zeta_3) &= \zeta_1(2\zeta_1-1) \\ N_2(\zeta_1,\zeta_2,\zeta_3) &= \zeta_2(2\zeta_2-1) \\ N_3(\zeta_1,\zeta_2,\zeta_3) &= \zeta_3(2\zeta_3-1) \\ N_4(\zeta_1,\zeta_2,\zeta_3) &= 4\zeta_1\zeta_2 \\ N_5(\zeta_1,\zeta_2,\zeta_3) &= 4\zeta_2\zeta_3 \\ N_6(\zeta_1,\zeta_2,\zeta_3) &= 4\zeta_1\zeta_3.\end{aligned} \tag{19}$$

A quadratic ansatz (Eq. (5)) has been used in the present calculation (see Sect. 5). The usefulness of higher degree polynomials will be discussed in a subsequent paper [17].

2.3. Matrix elements for the Schrödinger equation

For the calculation of the matrix element in Eq. 4 we express φ, $\delta\varphi$ and the potential energy $V(x, y)$ by formfunctions $N_i(\zeta_1, \zeta_2, \zeta_3)$. Because the expansion leads to matrices (6×6 for a quadratic polynomial) we express them in the bra-ket notation [9]

$$\begin{aligned}\varphi &= \langle \boldsymbol{N} | \boldsymbol{\varphi}^{(e)} \rangle, & \delta\varphi &= \langle \boldsymbol{N} | \delta\boldsymbol{\varphi}^{(e)} \rangle \\ \frac{\partial\varphi}{\partial x} &= \left\langle \boldsymbol{\varphi}^{(e)} \middle| \frac{\partial \boldsymbol{N}}{\partial x} \right\rangle, & \frac{\partial\varphi}{\partial y} &= \left\langle \boldsymbol{\varphi}^{(e)} \middle| \frac{\partial \boldsymbol{N}}{\partial y} \right\rangle \\ V(x,y) &= \langle \boldsymbol{N} | \boldsymbol{V}^{(e)} \rangle, & \boldsymbol{V}^{(e)} &= (V_1^{(e)}, V_2^{(e)}, \ldots, V_6^{(e)}).\end{aligned} \tag{20}$$

In case of a nonlinear coordinate transformation the kinetic energy operator includes coordinate dependent prefactors $f(x, y)$. Then these may be approximated by the polynomial expansion. As mentioned above the potential energy is also approximated by a polynomial where the exact values $V_i^{(e)}$ are given at the knots i. The contributions of each element to the whole domain G may be written in the following form:

$$\delta L_e = \langle \delta \boldsymbol{\varphi}^{(e)} | \boldsymbol{H}^{(e)} - E\boldsymbol{S}^{(e)} | \boldsymbol{\varphi}^{(e)} \rangle, \tag{21}$$

with $\boldsymbol{S}$ and $\boldsymbol{H}$ matrices

$$\boldsymbol{H}^{(e)} = \boldsymbol{T}^{(e)} + \boldsymbol{V}^{(e)} \tag{22}$$

$$\boldsymbol{T}^{(e)} = \int_{G_e} \left(\left| \frac{\partial \boldsymbol{N}}{\partial x} \right\rangle \left\langle \frac{\partial \boldsymbol{N}}{\partial x} \right| + \left| \frac{\partial \boldsymbol{N}}{\partial y} \right\rangle \left\langle \frac{\partial \boldsymbol{N}}{\partial y} \right| \right) \mathrm{d}G_e \tag{23}$$

$$\boldsymbol{V}^{(e)} = \int_{G_e} |\boldsymbol{N}\rangle \langle \boldsymbol{V}^{(e)} | \boldsymbol{N} \rangle \langle \boldsymbol{N}| \, \mathrm{d}G_e.$$

These are all 6×6 matrices.

Summing up these matrices a matrix of the size of the whole number of grid points N is build up. The final $N \times N$ matrix equation to be solved is

$$\boldsymbol{H}\boldsymbol{\phi} = E\boldsymbol{S}\boldsymbol{\phi}. \tag{24}$$

For asymptotic boundary conditions in scattering problems, one has to treat a linear equation with inhomogenity $\boldsymbol{F}$ and continuous scattering energy E

$$(\boldsymbol{H}' - E\boldsymbol{S}')\boldsymbol{\phi}' = \boldsymbol{F} \tag{25}$$

instead of the eigenvalue equation (24).

Finally we want to comment on the explicit calculation of matrix elements. The kinetic energy operator contains terms like

$$\left(\frac{\partial}{\partial x}\right)^2, \frac{\partial}{\partial x} \cdot \frac{\partial}{\partial y}, f(x, y) \cdot \left(\frac{\partial}{\partial x}\right)^2, \text{ etc.}$$

One first transforms to the natural coordinates, for example

$$\boldsymbol{N}_x = \frac{\partial \boldsymbol{N}}{\partial x} = \sum_{l=1}^{3} \frac{\partial \zeta_l}{\partial x} \frac{\partial \boldsymbol{N}}{\partial \zeta_l}. \tag{26}$$

Each matrix element T_{ij} consists of terms of the type

$$T_{ij} = \int_{G_e} (N_x^i N_x^j + \cdots) \, \mathrm{d}G_e \tag{27}$$

where the N's are polynomials of a given degree. The prototype integrals are once solved by hand for simple formfunctions. These prototype matrix elements are tabulated for $T^{(e)}$, $V^{(e)}$ and $S^{(e)}$ in the paper of Askar et al. [9b].

If the formfunctions are more complicated or if the kinetic energy includes coordinate dependent prefactors, then it is hardly possible to derive analytical formulas for all the integrals. For this purpose a small program was developed which calculates all prototype matrix elements for given formfunctions and operators.

Including also curvilinear elements (i.e. for a circle), this kind of procedure becomes also very core space or file space consuming. This means that the cartesian coordinates have to be expressed by formfunctions N, too

$$x = \boldsymbol{x}^T \cdot \boldsymbol{N}(\xi, \eta), \qquad y = \boldsymbol{y}^T \cdot \boldsymbol{N}(\xi, \eta). \tag{28}$$

In this case there may be too many prototype matrix elements, and the best way for integration is by some kind of Gaussian integration. In case of a unit triangle the general form is [5b]

$$\int\int_{G_0} \psi(\xi, \eta)\, \mathrm{d}\xi\, \mathrm{d}\eta = \sum_{i=1}^{m} \psi(\xi_i, \eta_i)\omega_i \tag{29}$$

with integration points ξ_i, η_i and weights ω_i. To our knowledge useful integration procedures exists only for a triangle with up to 13 grid points which are accurate for polynomials up to the ninth degree. Therefore, in Eq. (29) we can use formfunctions up to the third degree (note that the potential energy integral includes three times the formfunction). For higher order formfunctions and especially for curvilinear elements there seems to be so for no useful simple exact integration formula.

3. The calculation of the scattering matrix S

For the calculation of the S-matrix and the transition probability P in elastic, inelastic and reactive scattering one has to solve the problem in two stages. First we have to calculate the stationary wavefunction inside our boundaries and then to match the wavefunction at the boundary (logarithmic boundary condition [18]) to the exact asymptotic solution of the Schrödinger equation:

$$\phi_l = \kappa_l(y) \exp(-ik_x x) + \sum_{n=0}^{N_v} \left(\frac{k_l}{k_n}\right)^{1/2} S_{ln} h_l \kappa_n(y) \exp(ik_x x). \tag{30}$$

N_v is the number of open channels, κ_n are the eigenfunctions of the hamiltonian for coordinate y and eigenvalue ε_n. The wavevector is $k_i = (2\mu[E - \varepsilon_i])^{1/2}$ and E is the scattering energy. h_l describes whether the channel is open or closed ($h_l = 1$ or 0, resp.). The transition probability is

$$P_{ln} = |S_{ln}|^2. \tag{37}$$

The current conservation requires

$$\sum_n |S_{ln}|^2 = 1. \tag{32}$$

The matching procedure has been described by many authors, so we give only a brief survey. Our calculated stationary wavefunctions φ_α with special boundary condition α can be asymptotically written as

$$\varphi_\alpha = \sum_{n=1}^{M} (A_{\alpha n} \cos(k_n \xi) + B_{\alpha n} \sin(k_n \xi)) \kappa_n(\eta) \tag{33}$$

and have to be compared with Eq. (30). ξ, η are the internal orthogonal coordinates. φ_α is a linear combination of M asymptotic vibrational functions $\kappa_n(\eta)$ at the boundaries. The unknown translational part with coefficients $A_{\alpha n}$ and $B_{\alpha n}$ has to be determined and the coefficients are given as

$$A_{\alpha n} = \langle \kappa_n | \varphi_\alpha \rangle$$
$$B_{\alpha n} = \left\langle \kappa_n \left| \frac{\partial \varphi_\alpha}{\partial \xi} \right\rangle k_n^{-1} \right. \tag{34}$$

at the boundary $\xi = 0$ [9b].

The complex S-matrix results from

$$\boldsymbol{S} = \boldsymbol{h}\boldsymbol{Z}^{*-1}\boldsymbol{Z}\boldsymbol{h} \tag{35}$$

with

$$Z_{\alpha n} = \tfrac{1}{2}(A_{\alpha_n} - iB_{\alpha n})k_n^{1/2}. \tag{36}$$

The matrix elements S_{ij} or P_{ij} describe the probability of transition from state i to state j. The h-matrix ($h_{ij} = \delta_{ij}$) has been introduced to project out the closed channels, thus for a complete solution of the S-matrix we need as many linear independent boundary conditions as we have open channels for a given scattering energy.

Concerning the coefficients $A_{\alpha n}$ we use the orthonormality of the eigenfunctions $\{\kappa_n\}$, which results into $A_{\alpha n} = +1, -1$ or 0. The $B_{\alpha n}$ are calculated by numerical integration of Eq. (34b). The $\partial \varphi_\alpha / \partial \xi$ may be determined numerically or according to

$$\frac{\partial \varphi_\alpha^{(e)}}{\partial x} = \sum_{i=1}^{6} \frac{\partial N_i}{\partial x} \varphi_\alpha^{(e)}. \tag{37}$$

4. The structure of the FEM code for the Cyber 205

Our finite element code is especially adapted to the vector computer Cyber 205. For the chosen physical problems we need high accuracy and accordingly many grid points (1000 or much more), which results in a long vector length. This allows optimal vector coding, keeping the computing time short. Scalar machines are useful for small matrices and this may be the reason why FEM has not been used too often to answer quantum mechanical questions.

We have developed a program for different kinds of mathematically two-dimensional problems in inelastic and reactive scattering and bound state systems. The code was tested by recalculating results for inelastic scattering using different model potentials [19] and for reactive scattering by using the L-shape potential [20]. In the next section we will discuss in detail our results for the collinear hydrogen isotope reactions using the Porter and Karplus surface [21].

Before that some insight into the special features of the program and the Cyber 205 Fortran will be given. The Cyber 205 is a pipeline machine and works

efficiently for large vector lengths ($N \geq 200$). FEM needs simple matrix algebra. But because of the short bandwidth (i.e. 100–250, see Table 1) of the large matrices ($N = 6000$–$30\,000$) it was not easy to vectorize the matrix operations optimally, partly because the $\frac{1}{2}$ Mword main memory of the Cyber 205 in Bochum was too small. For an improved vectorisation it is advantageous to have a large core memory of at least 1.5 Mwords. In this case a Mflop rate between 20–50 can be reached.

The calculation of the integrals (Eq. 16) and the building up of the matrix $(\boldsymbol{H} - E\boldsymbol{S})$ (Eq. (25)) do not need much time compared to solving the linear equations with several boundary conditions. The analysis of the stationary states for calculating the transition probability is again negligible in time. The solution of the linear equation is achieved by two different methods, (a) the direct Cholesky method [5b] and (b) the iterative conjugate gradient method [5b] (see also appendix A). In the Cholesky method a decomposition of the matrix $\boldsymbol{A}$ in two triangular matrices $\boldsymbol{A} = \boldsymbol{L} \cdot \boldsymbol{L}^T$ is used. This triangularisation is the time consuming step. This step has to be done only once for different boundary conditions $\boldsymbol{F}$ (see Eq. (25)). The stationary solution $\boldsymbol{X}$ in $\boldsymbol{AX} = \boldsymbol{F}$ can be obtained easily. Having enough information about the energy dependence of the wavefunction one can use an iterative method with good starting vectors.

The special details of the numerical procedures will be published elsewhere [22], some important aspects being given in appendix A. For the Cholesky procedure we still don't have the optimum code, because the Cholesky algorithm needs the values of the matrix recursively. This complicates vectorisation. The vector length is here equal to the half-bandwidth of the matrix $\boldsymbol{A}$ and only for large dimensions of $\boldsymbol{A}$ this can be greater than 200.

The iterative procedure can be vectorized optimally. The vector length can be as long as the dimension of $\boldsymbol{A}$. To keep the number of iterations as small as possible, one has to search for efficient convergence procedures.

Table 1. CPU-time (sec) for Cholesky and conjugate gradient methods (N = number of grid points, M = half-bandwidth)

		Cholesky[a]		Conjugate gradient[b]	
N	M	A	B	A	B
6201	116	6.7	0.6	0.07	
9751	146	14.1	1.0		0.22
14 101	176	25.2	1.8		0.32
19 251	206	44.4	2.9		0.44
25 201	236	70.4	4.4		0.57
31 951	266	105.7	6.2		0.72

[a] Part A: triangularisation, part B: forward and backward substitution; time includes CPU-time for I/O, too

[b] Time for one iteration (A: fastest version, long vector length; B: compact version, very short vector length, not optimized)

The calculation of the scattering matrix for different energies needs the hamilton- and overlap-matrix (Eqs. (22), (23)) only once. In case of direct solution for each scattering energy the decomposition of the matrix $(\boldsymbol{H}-E\boldsymbol{S})$ is solved once, and for each boundary condition a stationary solution has to be calculated. Only the partitioning of the matrix takes a large amount of computer time (i.e. like the inversion of a matrix), the time for the different boundary conditions is then negligible.

Representative CPU-times are given in Table 1.

5. The isotope reaction $H+H_2$

5.1. Introduction

In the last ten to twenty years many methods have been developed for exactly solving low dimension (D = 1, 2, 3) scattering problems. In the beginning the finite difference method and different forms of close coupling type procedures were used. But since the early beginning finite differences could not really compete with the today nearly standard methods like conventional *R*-matrix [23] or hyperspherical coordinate methods using *S*-matrix or *R*-matrix propagation [24–28, 41, 42]. The test example for all these methods is the collinear $H+H_2$ reaction.

With FEM we investigated the $H+H_2$ reaction and their isotopes using the Porter-Karplus potential surface [21]. Our aim is to show that FEM can be used for different situations with light (L) and heavy (H) atoms:

(a) symmetric and asymmetric reactions
(b) small skew angle and large skew angle (i.e. HLH or LHL systems) and
(c) cases with many open channels.

The light (L) and heavy (H) atoms in our collinear reactions are H, D, T, Mu. Since our final aim is the treatment of 3D scattering, the first step is to solve the 2D problem in comparatively short time.

For the solution of the reaction $A+BC \rightarrow AB+C$ we used mass-weighted coordinates. Usually the kinetic energy is expressed by the new coordinates Z_1 and Z_2, related to the interparticle distances r_{AB} and r_{BC}:

$$Z_1 = r_{AB} + [m_C/(m_B+m_C)]r_{BC}$$

$$Z_2 = \sqrt{\frac{m_{BC}}{m}}\, r_{BC};$$

$$m = m_A(m_B+m_C)/(m_A+m_B+m_C)$$

$$m_{BC} = m_B m_C/(m_B+m_C)$$

such that a simple diagonal kinetic energy results

$$T = \frac{1}{2m}\left(\frac{\partial^2}{\partial Z_1^2}+\frac{\partial^2}{\partial Z_2^2}\right).$$

The introduction of these reduced mass-weighted coordinates results in a potential surface with a skew angle α as shown in Fig. 3. Its form explains some dynamical aspects (i.e. whether vibrational, rotational or translational energy is important). On the other hand the size of the 2D surface can be enlarged by the transformation considerably, which may result in numerical difficulties.

5.2. $H+H_2$

In the case of $H+H_2$ ($m_H = 1.00797$) α is 60°. The symmetric potential area was discretized into a certain number of finite elements and we increased the number of grid points in order to find convergent results. The range for the coordinates Z_1 and Z_2 is given by (see Fig. 3) $Z_1 \approx 1.5\text{-}7.0a_0$, $Z_2 \approx 0.6\text{-}5.5a_0$. This range of Z_1 and Z_2 corresponds to $r_{H_2} \approx 0.5\text{-}6.0a_0$. The asymptotic part for large Z_1 corresponds to $Z_2 \approx 0.6\text{-}2.4a_0$.

The boundary values for the asymptotes are the eigenfunctions of the diatomic Morse oscillator (H_2 [21]: $D_e = 4.7466$ eV, $R_e = 1.40083a_0$, $\beta = 1.04435a_0$).

In Fig. 4 we show the reaction probabilities for $H+H_2$ ($v=0$) $\rightarrow H_2$ ($v'=0$) $+H$ with up to 3 open vibrational channels and compare it with the work of Römelt [27] and with other close coupling type results [24–38]. As can be seen our results exactly agree with the values from the literature.

The calculations in Fig. 4 were done for $K = 5000$ finite elements and $N = 10\,251$ grid points (this number of elements has been proved to give convergent results as reported below). Although it is possible to use the time saving Richardson extrapolation [39] in FEM, it was not utilized here.

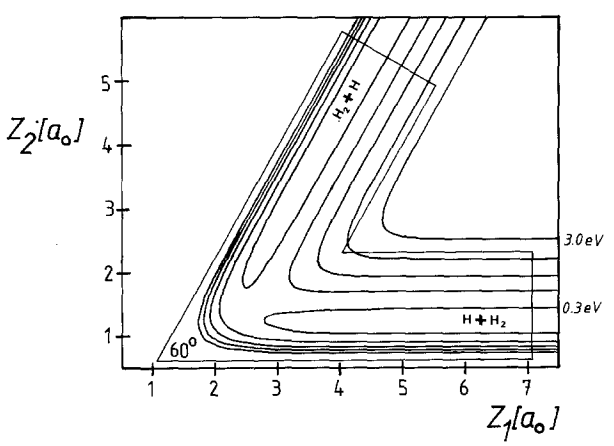

Fig. 3. The Porter-Karplus (PK) surface [21] plotted in mass weighted coordinates Z_1, $Z_2(a_0)$ for the collinear reaction $H+H_2$. The contours are drawn for $E = 0.3$, 0.975, 1.65, 2.325 and 3 eV. The v-shape section is the integration domain for our calculations with skew angle $\alpha = 60°$. The wavefunction at the entrance and exit channels are Morse-oscillator solutions, the wavefunction at the remainder of the boundary is set to zero

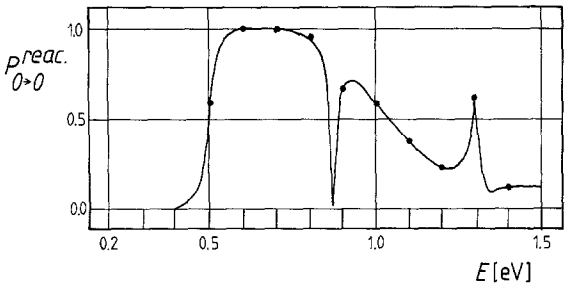

Fig. 4. The transition probability P_{00}^{reac} for the collinear $H+H_2\,(v=0)\to H_2\,(v'=0)+H$ reaction as a function of the total energy E. E is measured relative to the bottom of the reactant potential energy well. ——: results of Römelt [27] (agreeing with other literature results [24–38, 41]), ●: present results

In order to test the convergence we calculated the S-matrix at special energies for a different number of grid points. One result is shown in Table 2. As can be seen the convergence of the transition probability P is reached very early ($N_{grid} \leq 1700$), but the stationary wavefunction ($\partial\varphi/\partial n$) is still locally not correct. There are other systems where the convergence of P is much slower and the convergence of the correct phase of the wavefunction and of the transition probability are comparable (e.g. H+MuH). The necessary accuracy depends on the physical problem under investigation (e.g. H+MuH, $F+H_2$). Using many open states, one naturally has to include more points to describe the oscillations of the eigenfunctions accurately. For some systems (H+MuH, $F+H_2$) an increasing number of points in translational direction was needed. $H+H_2$ itself is a very simple and easy system, where one finds no complications.

Now our results are compared with a few previous results in detail. Römelt [27] (see Table 3) used the hyperspherical coordinate method including S-matrix propagation. According to the convergence tests the results are better than 1%, the difference between the nondiagonal values $P_{01}^{in,reac}$ and $P_{10}^{in,reac}$ values if of the order of 0.1% or even smaller. In many cases Römelts results agree with ours to within 1%, otherwise the results given here are probably more accurate.

In Table 4 we compare with the work of Rosenthal and Gordon [36] and of Diestler [38] were reaction probabilities for 3 open vibrational channels are given.

Table 2. Test of convergence for $H+H_2$ with $E=0.022$ au. Comparison of the transition probability P_{00}^{reac}, the integral $B_{\alpha n}$ ($\alpha=n=1$, Eq. 34) and the value of the normal derivative of ϕ_α ($\alpha=1$, Eq. 37) at R_e (H_2) at the entrance boundary

N_{grid}	$\frac{\partial\phi_1(\approx R_e)}{\partial n}$	B_{11}	P_{00}^{reac}
1701	8.91	5.202	0.99917
3751	7.33	4.331	0.99918
6601	6.85	4.203	0.99915
10 251	6.88	4.170	0.99913

Table 3. Inelastic and reactive collision probabilities for $H+H_2$ ($N_{grid}=10251$). The values in parentheses are from Römelt [27]

E (ev)	P_{00}^{in}	$P_{01/10}^{in}$	P_{11}^{in}	P_{00}^{reac}	$P_{01/10}^{reac}$	P_{11}^{reac}
0.4	0.99812 (0.998)			0.00188 (0.002)		
0.5	0.40834 (0.407)			0.59166 (0.593)		
0.6	0.00072 (0.003)			0.99928 (0.997)		
0.7	0.00862 (0.009)			0.99138 (0.991)		
0.8	0.04675 (0.049)	0.0 (0.017)	1.0 (0.965)	0.95325 (0.941)	0.00001 (0.004)	0.0 (0.0)
0.9	0.02879 (0.031)	0.11734 (0.120)	0.39846 (0.409)	0.67774 (0.676)	0.17642 (0.177)	0.30807 (0.299)
		0.11710			0.17608	
1.0	0.07471 (0.079)	0.08639 (0.082)	0.15946 (0.162)	0.59865 (0.591)	0.23925 (0.245)	0.51390 (0.509)
		0.08704			0.24059	
1.1	0.14613 (0.151)	0.13838 (0.138)	0.14350 (0.143)	0.38768 (0.388)	0.32797 (0.327)	0.39031 (0.394)
		0.13832			0.32771	
1.2	0.19196 (0.200)	0.22183 (0.219)	0.18541 (0.183)	0.23284 (0.234)	0.35390 (0.353)	0.23939 (0.249)
		0.22150			0.35316	
1.3	0.01711 (0.023)	0.28568 (0.280)	0.44919 (0.452)	0.62455 (0.621)	0.07163 (0.077)	0.19269 (0.185)
		0.28521			0.07166	
1.4	0.25264 (0.270)	0.21324 (0.190)	0.12479 (0.121)	0.13159 (0.127)	0.25057 (0.256)	0.24923 (0.250)
		0.21326			0.25023	

Table 4. Reactive collision probabilities P^{reac} for collinear $H + H_2$[a]. 1st line: present results, 2nd line: Rosenthal and Gordon [36], 3rd line: Diestler [38]

N_{grid}	E_{tot} (eV)	P_{00}	P_{01}	P_{10}	P_{11}	P_{02}	P_{20}	P_{12}	P_{21}	P_{22}
6601	0.4826	0.376								
		0.372								
		0.366								
6601	0.5376	0.918								
		0.916								
		0.910								
6601	0.8426	0.852	0.00303	0.00312	0.00020					
		0.858	0.00238	0.00239	0.00015					
		0.853	0.003	0.003	0.00020					
10251	1.2966	0.562	0.110	0.110	0.150	0.3 (−3)	0.24 (−3)	0.22 (−3)	0.27 (−3)	<0.1 (−4)
		0.663	0.070	0.070	0.214	0.95 (−4)	0.14 (−3)	0.47 (−4)	0.44 (−4)	0.32 (−7)
		—	—	—	—	—		—	—	—
10251	1.4466	0.135	0.216	0.217	0.225	0.100	0.101	0.138	0.138	0.530
		0.153	0.233	0.236	0.198	0.086	0.088	0.120	0.121	0.530
		—	—	—	—	—	—	—	—	—
10251	1.5466	0.120	0.153	0.153	0.202	0.126	0.125	0.179	0.178	0.396
		0.135	0.167	0.169	0.200	0.124	0.127	0.150	0.152	0.397
		—	—	—	—	—	—	—	—	—
10251	1.6466	0.078	0.103	0.103	0.210	0.137	0.137	0.186	0.186	0.185
		0.069	0.125	0.126	0.227	0.179	0.182	0.141	0.141	0.137
		—	—	—	—	—	—	—	—	—
6601	1.6466	0.082	0.105	0.106	0.210	0.141	0.141	0.184	0.185	0.185

[a] Values in parentheses are powers of 10

Table 5. Reactive probabilities P^{reac} for collinear $H+H_2$ with five open channels

N_{grid}	E (eV)	P_{00}	P_{11}	P_{22}	P_{33}	P_{44}
10 251	2.1	0.02711	0.07668	0.18616	0.09484	0.0
	2.2	0.02385	0.18293	0.06564	0.47164	0.00042
	2.3	0.01580	0.06601	0.12057	0.12356	0.54358
	2.4	0.00995	0.05451	0.12609	0.08476	0.48478
14 701	2.4	0.00925	0.05245	0.12414	0.08578	0.48333

For convergence tests we also present results for different numbers of grid points. The agreement is less impressive than in Table 3. Small differences may partly result from slightly different conversion factors and mass units. The present results are very near to convergence (except for the highest energies).

In Table 5 reaction probabilities for five vibrational states are given for several energies. There is good agreement with the curves shown in the paper of Kuppermann [25] except for P_{44}, where Kuppermann's values are roughly 20% too small.

5.3. The symmetric reactions H+DH, D+HD *and* H+MuH

We now investigate the capability of FEM for some symmetric isotopic reactions, namely H+DH, D+HD and H+MuH. The present reaction probability P_{00}^{reac} of HDH and DHD can be found in excellent agreement with the results of Kuppermann [25] which can be seen in Figs. 5 and 6. The calculations were performed with 6601 grid points where convergent results can be expected for energies for at least up to 1 eV. In addition we list in Table 6 the total reaction probabilities $P_{0\to n}^{reac}$ for different reactions including HDH and DHD. The results in Table 6 are compared with the early work of Wu et al. [31]. In most cases our results are accurate within a few tenth of a percent.

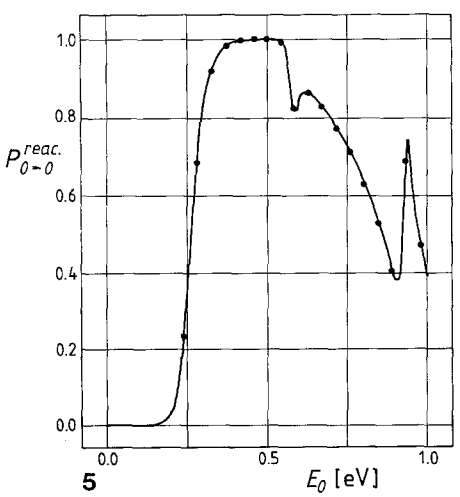

Fig. 5. The reaction probability P_{00}^{reac} for the collinear exchange reaction H+DH ($v=0$)→ HD ($v'=0$)+H on the PK surface. E_0 is the initial relative translational energy. ——: results of Kuppermann [25], ●: present results

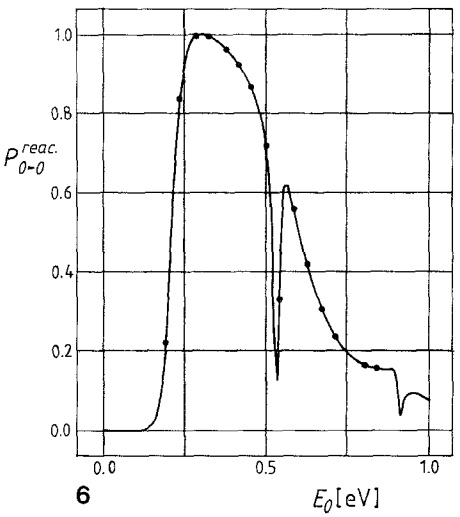

Fig. 6. The reaction probability P_{00}^{reac} for the collinear exchange reaction D+HD ($v=0$)→ DH ($v'=0$)+D on the PK surface. E_0 is the initial relative translational energy. ——: results of Kuppermann [25], ●: present results

Table 6. Sum of reaction probabilities $\Sigma_n P_{0\to n}^{reac}$ for different isotope reactions. The first numbers are present results and the values in parentheses are from Wu et al. [31][a]

E (kcal/mol)	D+H_2	H+D_2	H+DH	D+HD
7.0	0.0	0.0	0.0	0.0
8.0	10^{-5} (0.0)	0.00004 (0.0)	0.00002 (0.0)	0.0001 (0.0)
9.0	0.002 (0.001)	0.002 (0.002)	0.001 (0.001)	0.009 (0.010)
10.0	0.059 (0.057)	0.047 (0.046)	0.027 (0.026)	0.214 (0.222)
11.0	0.469 (0.465)	0.341 (0.344)	0.237 (0.231)	0.832 (0.843)
12.0	0.879 (0.877)	0.770 (0.775)	0.690 (0.865)*	0.996 (0.997)
13.0	0.968 (0.967)	0.940 (0.938)	0.916 (0.921)	0.993 (0.991)
14.0	0.978 (0.976)	0.979 (0.978)	0.982 (0.980)	0.966 (0.966)
15.0	0.970 (0.969)	0.986 (0.986)	0.995 (0.995)	0.923 (0.928)
16.0	0.951 (0.950)	0.966 (0.964)	0.999 (0.999)	0.862 (0.861)
17.0	0.914 (0.912)	0.839 (0.838)	1.0 (1.0)	0.717 (0.710)
18.0	0.818 (0.809)	0.769 (0.771)	0.997 (0.997)	0.610 (0.643)*
19.0	0.906 (0.907)	0.894 (0.894)	0.945 (0.944)	0.687 (0.685)
20.0	0.942 (0.936)	0.962 (0.960)	0.982 (0.981)	0.563 (0.655)*
21.0	0.820 (0.814)	0.951 (0.950)	0.986 (0.986)	0.470 (0.477)
22.0	0.715 (0.702)	0.918 (0.914)	0.984 (0.985)	0.408 (0.416)
23.0	0.649 (0.631)	0.808 (0.801)	0.980 (0.979)	0.365 (0.375)
24.0	0.591 (0.574)	0.665 (0.660)	0.968 (0.968)	0.339 (0.476)*
25.0	0.548 (0.535)	0.697 (0.697)	0.945 (0.943)	0.308 (0.321)

[a] Values with an asterisk may be misprints or are near a resonance

The calculations are comparably easy for large skew angles, i.e. comparable masses. In the case of H+MuH we get a small skew angle $\alpha = 26.1°$ and a correspondingly large integration area in mass-weighted coordinates. Therefore we expect less accurate results for a given number of grid points. It was necessary to shift the asymptotic boundary further out to larger atom-molecule distances than used for $H+H_2$, because the transition probabilities were more sensitive to the position of the boundary ($Z_1 \approx 2.0 - 13.0a_0$; for $Z_1 = 13.0a_0$: $Z_2 \approx 0.15 - 1.53a_0$). First comparison with the calculations of Manz and Römelt (MR) [40] seemed to be disappointing. The small mass differences (MR: $m_H = 1.008$ amu, $m_{Mu} = \frac{1}{9}m_H$; present calc.: $m_H = 1837.109$ emu $= 1.00797$ amu, $m_{Mu} = 207.768$ emu $= 1/8.842\, m_H$) lead to large differences for some individual reaction transition probabilities, e.g. P_{00}^{reac}, as can be seen in Fig. 7. In order to compare with the MR values we used $m_H = 1.00797$ amu and $m_{Mu} = \frac{1}{9}m_H$. The results (Table 7 and Fig. 7) are now in good agreement with MR [40, 28]. Between the two calculations small differences in masses and conversion factors still may exist, resulting in some discrepancies, namely ~10% for P_{00}^{reac}. For energies $E > 2.6$ eV the results with 32 851 grid points are nearly convergent. This number of grid points seems to be very large. If one exploits symmetry, only half of the points would be needed. Using polynomials of higher degree a considerable reduction of points can be expected. The question still remains, if the use of the internal coordinates with nondiagonal terms in the kinetic energy would lead to convergent results at a reduced number of grid points.

5.4. *The asymmetric reactions* $Mu+D_2$, $H+D_2$, $D+H_2$

As in the case of the symmetric reactions in Sect. 5.3, we used only $N = 6601$ grid points for these asymmetric reactions, and expect no problems up to the first four open channels.

Results are given for $Mu+D_2$ (Fig. 8) and for $Mu+D_2$, $H+D_2$ and $D+H_2$ (Tables 6, 8). For these systems the integration area of the mass-weighted coordin-

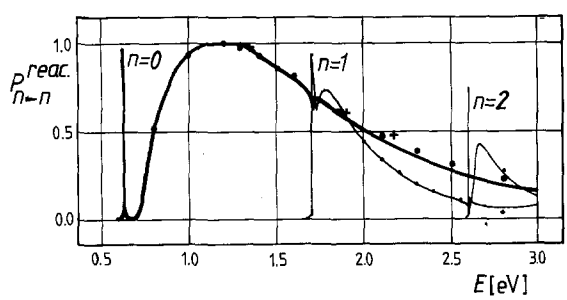

Fig. 7. The reaction probabilities $P^{reac}_{n\to n'}$ for the collinear reaction $H+MuH(n) \to HMu(n')+H$ ($n = n' = 0, 1, 2$) on the PK-surface as function of total energy E. E is measured relative to the bottom of the reactant potential energy well. ——: *MR* [40] results, ●: present results ($m_H = 1837.109$ emu, $m_{Mu} = 1/9\, m_H$). +: results from calculations with slightly different masses ($m_H = 1837.109$ emu, $m_{Mu} = 1/8.842\, m_H$) but with equivalent accuracy

Table 7. Reactive probability P^{reac} for collinear H+MuH[a]. The values in parentheses are from Manz and Römelt [40]

N_{grid}	E(eV)	P_{00}	P_{01}	P_{11}	P_{02}	P_{12}	P_{22}
14 101	0.8	0.514 (0.516)					
14 101	1.0	0.934 (0.937)					
14 101	1.2	0.997					
19 251		0.997 (0.996)					
19 251	1.3	0.972					
25 201		0.970 (0.997)					
19 251	1.4	0.928					
25 201		0.924 (0.918)					
19 251	1.5	0.874					
25 201		0.868 (0.857)					
19 251	1.6	0.823					
25 201		0.814 (0.800)					
25 201	1.7	0.679	0.029	0.009			
31 951		0.686 (0.667)	0.017 (0.018)	0.217 (0.221)			
31 951	1.9	0.594 (0.569)	0.014 (0.016)	0.583 (0.576)			
31 951	2.1	0.481 (0.450)	0.017 (0.017)	0.348 (0.347)			
31 951	2.3	0.388 (0.355)	0.017 (0.013)	0.200 (0.198)			
31 951	2.5	0.315 (0.275)	0.015 (0.009)	0.102 (0.119)			
31 951	2.6	0.283 (0.247)	0.015 (0.005)	0.073 (0.097)	0.003 (0.000)	0.003 (0.004)	0.057 (0.061)
31 951	2.8	0.232 (0.198)	0.012 (0.003)	0.025 (0.070)	0.003 (0.000)	0.001 (0.003)	0.283 (0.258)
31 951	3.0	0.193 (0.159)	0.009 (0.001)	0.005 (0.085)	0.000 (0.000)	0.000 (0.001)	0.110 (0.123)

[a] In the present calculation: $m_H = 1837.109$ emu, $m_{Mu} = 1/9 m_H$, so that the results are fairly comparable with [40]

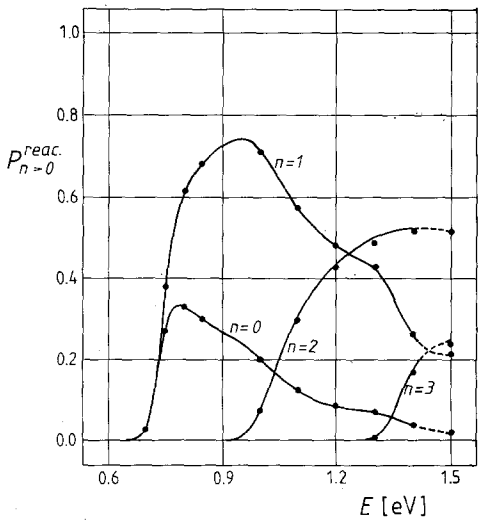

Fig. 8. Collinear initial-state-selected reaction probabilities $P^{reac}_{n\to 0}$ for the $Mu+D_2$ reaction as function of total energy E. E is measured relative to the bottom of the reactant potential energy well. ——: results of Bondi et al. [41], ●: present results

ates is only slightly larger than for $H+H_2$. Therefore we expect the same accuracy as for $H+H_2$.

Some results for $Mu+D_2$ are given in Table 8 and are compared with the work of Bondi et al. [41] in Fig. 8. For $H+D_2$ and $D+H_2$ the presęnt results are compared with the work of Wu et al. [31] in Table 6. The agreement is excellent.

6. Discussion and conclusion

As has been shown before by Askar et al. [9] FEM is a very useful and accurate method for solving reactive scattering problems in 2 dimensions. The idea of using piecewise local functions in scattering theory is not new [23, 36, 43]. It is mostly used for the propagation of the wavefunction, but with FEM we can calculate the whole scattering wavefunction in one step. This global type of the

Table 8. Reaction probabilities for collinear $Mu+D_2$ ($v=0, 1, 2, 3$) → $MuD(v=0)+D$[a]

E (ev)	P^{in} (MuD)	P^{reac}_{00} (MuD)	10	20	30
0.7	0.938	0.034	0.030	—	—
0.75	0.336	0.278	0.386	—	—
0.8	0.052	0.333	0.616	—	—
0.85	0.013	0.303	0.685	—	—
1.0	0.004	0.207	0.712	0.076	—
1.1	0.003	0.128	0.575	0.295	—
1.2	0.002	0.091	0.486	0.420	—
1.3	0.003	0.075	0.432	0.484	0.005
1.4	0.003	0.041	0.268	0.516	0.172
1.5	0.001	0.029	0.216	0.510	0.243

[a] Number of grid points: $N=6601$

FEM procedure allows to obtain realistic estimates of the accuracy and convergence properties.

Our aim is the systematic investigation of the usefulness of FEM for dynamical problems, and for electronic structure calculations, too. In the work we tried to show that by using a modern vector computer like the Cyber 205 mathematical two-dimensional scattering problems can be solved in reasonable times. We gave a first overview of our work, where we calculated reaction probabilities for the hydrogen isotope reactions including symmetric and asymmetric configurations and including up to five open vibrational states for each channel.

In the present calculations we did not make use of the symmetry of the potential surface, so that one can directly compare symmetric and asymmetric cases. For the local wavefunctions in FEM a simple approximation was used: the quadratic polynomial. The inclusion of symmetry and of polynomials of higher degree with explicit derivatives will cut down the number of necessary grid points considerably. We hope that this results in a large decrease of computing time for solving the linear equations.

The FEM code for the present calculations is still not optimal compared to the standards in engineering science today. The small bandwidth of the matrix resulting from optimal numbering of the nodes can be improved and the discretization into elements has not been optimally adapted to the chosen physical problem. We think that these improvements will probably result into a further reduction of computer time making FEM more competitive in comparison to conventional basis set expansion methods. There may still be problems left, where conventional methods seem to be more useful (e.g. resonances). But it is not clear whether these problems are relevant in higher dimensions.

The general complexity will increase for higher dimensions. We have started to develop a FEM code for three dimensions. 3D investigations are done by Kuppermann and Hipes [12] and Linderberg et al. [11] for $H+H_2$ by propagating the two-dimensional eigenfunctions (calculated by FEM) in the conventional way (i.e. R-matrix). Recently a new quantum mechanical approach using L^2 basis sets for solving 3D reactive scattering problems ($D+H_2$ ($v=1$)) has been published [46].

We are going to do similar calculations with FEM in full three dimensions, which seems to be a feasible project on the basis of the present experience.

Appendix A: The Cholesky and conjugate gradient method for solving the linear equation $Ax = b$

(a) Cholesky method [5b, 44]

In the Cholesky method, which is normally used for symmetric and *positive definite* matrices, first a symmetric decomposition into a lower-triangular matrix L is performed;

$$A = LL^T.$$

Then, using the process of forth-and-back substitution one solves the equation

$$\boldsymbol{L}\boldsymbol{L}^T\boldsymbol{x}-\boldsymbol{b}=0.$$

In textbooks [5b] the Cholesky method is described only for positive definite matrices. We now give the algorithm as it is used in our FEM program for a symmetrical nonpositive definite band matrix (m = semibandwidth) with the convention that L_{pq} is zero if $q \leqslant 0$ or $q > p$:

$$A_{ij}=0 \quad \text{for } (|i-j|)>m$$

$$L_{ij}=\begin{cases}\left(A_{ij}-\sum_{k=i-m}^{i-1} L_{ki}L_{kj}S_k\right)\Big/ L_{jj}; & j=i-m,\ldots,i-1;\ i=1,\ldots,n\\ 0 \quad \text{for } i-j>m\end{cases}$$

$$M_i=A_{ii}-\sum_{k=1}^{i-1} L_{ik}^2 S_k; \qquad i=1,\ldots,n$$

$$S_i=\operatorname{sign}(M_i)$$

$$L_{ii}=\sqrt{|M_i|}\cdot S_i.$$

In case of a nonpositive definite matrix diagonal matrix-elements L_{ii} will become imaginary, leading to a complex matrix $\boldsymbol{L}$. This problem is handled by storing the information whether L_{ii} is real or imaginary in a bit vector S_i.

In general m is much smaller than n. There are then approximately $n\times(m+1)\times(m+2)$ additions, $n\times(m+1)\times(m+2)$ multiplications and n square roots, signs and absolute values in the decomposition. Only the summation part can be "vectorized" (Q8SDOT), because the algorithm is recursive.

The solution of the set of equations $\boldsymbol{A}\boldsymbol{x}=\boldsymbol{b}$ can be performed in two steps

$$(1)\ \boldsymbol{L}\boldsymbol{c}=\boldsymbol{b}, \qquad (2)\ \boldsymbol{L}^T\boldsymbol{x}=\boldsymbol{c}$$

where we have introduced $\boldsymbol{c}=\boldsymbol{L}^T\boldsymbol{x}$:

$$c_i=\left(b_i-\sum_{k=i-m}^{i-1} L_{ki}c_kS_k\right)\Big/ L_{ii}; \qquad i=1,\ldots,n$$

$$x_i=\left(c_i-\sum_{k=i+1}^{i+m} L_{ik}x_k\right)\Big/ L_{ii}; \qquad i=n,\ldots,1.$$

Approximately $4n\times(m+1)$ multiplications and $2n\times(m+1)$ additions are involved in a solution and any number of right-hand sides can be processed when $\boldsymbol{L}$ is known.

In the Fortran code the elements for $\boldsymbol{L}$ and $\boldsymbol{c}$ are stored on $\boldsymbol{A}$ and $\boldsymbol{x}$. In case of very large matrices, where I/O for matrices $\boldsymbol{A}$ and $\boldsymbol{L}$ has to be included, the necessary working space for $\boldsymbol{A}$ and $\boldsymbol{L}$ need not be larger than $m\times(m+1)$.

At the moment we get a rate of roughly 20–50 MFLOP for the Cholesky method, which is fairly good.

(b) Conjugate gradient method

For the refinement of the Cholesky-solution and for problems with good starting vectors, we use the conjugate gradient (CG) method as an iterative method, first described by Hestenes and Stiefel [45, 5b]. The algorithm can be described in short as follows: starting with an initial guess x_0 two sequences of vectors $x_0, x_1, x_2, \ldots$ and $r_0, r_1, r_2, \ldots$ (residual vector: $r_k = Ax_k + b$) are generated iteratively by a special procedure, explained in detail in [5b]. This method can be vectorized optimally if we do not use sparse matrix techniques. The time consuming step in each iteration is the product $A \times x_k$. For the band matrix A we use the diagonal vector storage, which allows us to calculate the product $A \times x_k$ with vector operations of the length n, especially triadic operations, which are the fastest on the Cyber 205. A MFLOP-rate of ≈80 results. In case of small core memory a compact matrix A is used, leading to a less effective vectorization (see Table 1).

Acknowledgement. The author thanks Professors V. Staemmler, W. Kutzelnigg and W. H. E. Schwarz for their continuous encouragement and fruitful discussions. I also thank the Bochum-Theoretical Chemistry-group, especially U. Fleischer for valuable assistance. The computations have been carried out at the computer center of the Ruhr-Universität (Bochum).

References

1. Hockney RW, Jesshope CR (1981) Parallel computers. Hilger, Bristol
2. a. Dykstra CE (1984) Advanced theories and computational approaches to the electronic structure of molecules. NATO ASI Series C, vol. 133. Reidel, Dordrecht; b. Schaefer III HF (1977) Methods of electronic structure theory. Plenum Press, New York
3. a. Dupuis M (1986) Supercomputer simulations in chemistry. Lecture Notes in Chemistry, vol 44. Springer, Berlin Heidelberg New York; b. Kutzelnigg W, Schindler M, Klopper W, Koch S, Meier U, Wallmeier H: in [3a], p 55
4. a. Miller WH (1976) Dynamics of molecular collisions, Parts A and B. Plenum Press, New York; b. Clary DC (1986) The theory of chemical reaction dynamics. Reidel, Dordrecht; c. Truhlar DG (1981) Potential energy surfaces and dynamics calculations. Plenum Press, New York; d. Bernstein RB (1979) Atom-molecule collision theory. Plenum Press, New York; e. Baer M (1985) Theory of chemical reaction dyanmics, vol. I–IV. CRC Press, Boca Raton
5. a. Zienkiewicz OC (1971) The finite element method in engineering science. McGraw Hill, New York; b. Schwarz H R (1980) Methode der finiten Elemente. Teubner, Stuttgart; c. Bathe KJ, Wilson EL (1977) Numerical methods in finite element analysis. Prentice Hall, Englewood Cliffs, New Jersey; d. "Finite elements in physics", Graduate Summer course on Comp Physics, 1–10 Sept. 1986, EPF Lausanne, Org.: Gruber R
6. Askar A (1975) J Chem Phys 62:732
7. a. Nordholm S, Bacskay G (1976) Chem Phys Lett 42:253; b. Arai H, Kanesaka I, Kagawa Y (1976) Bull Chem Soc Jpn 49:1785
8. Friedmann F, Rosenfeld Y, Rabinovitch A, Thieberger R (1978) J Comput Phys 26:169
9. a. Rabitz H, Askar A, Cakmak A (1978) Chem Phys 29:61; b. Askar A, Cakmak A, Rabitz H (1978) Chem Phys. 33:267; c. Duff M, Rabitz H, Askar A, Cakmak A, Ablowitz M (1980) J Chem Phys 72:1543
10. a. Dilling W (1981) Diplomthesis, MPI, Göttingen; b. Barg GD, Askar A (1980) Chem Phys Lett 76:609; c. Love RB, Malik DJ (1985) Chem Phys 93:445
11. a. Mishra M, Linderberg J, Öhrn Y (1984) Chem Phys Lett 111:439; b. Linderberg J (1986) Int J Quantum Chem S19:467; c. Linderberg J, see [5d]; d. Linderberg J, Vessal B, Int J Quantum

Chem, accepted; e. Mishra M, Linderberg J (1983) Mol Phys 50:91; f. Linderberg J, Öhrn Y (1985) Int J Quantum Chem 27:273
12. a. Kuppermann A, Hipes P G (1986) J Chem Phys 84:5962; b. Hipes PG, Kuppermann A (1987) Chem Phys Lett 133:1
13. Christensen-Dalsgaard BL (1982) J Phys A: Math Gen 15:2711; (1984) Phys Rev 29:470
14. a. Levin FS, Shertzer J (1985) Phys Rev A32:3285; b. Ford WK, Levin FS (1984) Phys Rev A 29:43
15. Askar A, Rabitz H (1984) J Chem Phys 80:3586
16. Schulze W, Kolb D (1985) Chem Phys Lett 122:271
17. Jaquet R, to be published
18. Wigner EP, Eisenbud L (1947) Phys Rev 72:29
19. a. Diestler DJ, McKoy V (1968) J Chem Phys 48:2941; (1968) 48:2951; b. Connor JNL, Mayne MR (1976) Mol Phys 32:1123
20. Hirschfelder JO, Tang KT (1976) J Chem Phys 64:760
21. Porter RN, Karplus M (1964) J Chem Phys 40:1105
22. Ehlich H, Wojcieszynski B (1987) Proceedings of the 1986 Conferences on Cyber 200 in Bochum
23. Light JC, Walker RB (1976) J Chem Phys 65:4274
24. Kuppermann A, Kaye JA, Dwyer JP (1980) Chem Phys Lett 74:257
25. Kuppermann, A, in: [4c], p 375
26. Hauke G, Manz, J, Römelt J (1980) J Chem Phys 73:5040
27. Römelt J (1980) Chem Phys Lett 74:263
28. Römelt J (1983) Chem Phys 79:197
29. Manz J, Pollak E, Römelt J (1982) Chem Phys Lett 86:26
30. Bondi, DK, Connor JNL (1985) J Chem Phys 82:4383
31. Wu S, Johnson BR, Levine RD, (1973) Mol Phys 25:611
32. Johnson BR (1972) Chem Phys Lett 13:172
33. Duff JW, Truhlar DG (1973) Chem Phys Lett 23:327
34. Adams JT, Smith RL, Hayes EF (1974) J Chem Phys 61:2193
35. Truhlar DG, Wyatt RE (1976) Ann Rev Phys Chem 27:1
36. Rosenthal A, Gordon RG (1976) J Chem Phys 64:1641
37. Truhlar DG, Kuppermann A, Adams JT (1973) J Chem Phys 59:395
38. Diestler DJ (1971) J Chem Phys 54:4547
39. See discussion in [9c]
40. Manz J, Römelt J (1980) Chem Phys Lett 76:337
41. a. Bondi DK, Clary DC, Connor JNL, Garrett BC, Truhlar DG (1982) J Chem Phys 76:4986 b. Bondi DK, Connor JNL (1982) Chem Phys Lett 92:570
42. a. Lepetit B, Launay JM, Dourneuf M Le (1986) Chem Phys 106:103 and references therein; b. Launay JM, Dourneuf MLe (1982) J Phys B 15:L455
43. a. Sams WN, Kouri D J (1969) J Chem Phys 51:4809; b. Gordon R (1969) J Chem Phys 51:141; (1971) Methods Comput Phys 10:81
44. Wilkinson JH, Reinsch C (1971) Linear algebra. Handbook for automatic computation, vol. II. Springer, Berlin Heidelberg New York
45. Hestenes M, Stiefel E (1952) J Res Nat Bur Stand 49:409
46. Haug K, Schwenke DW, Shima Y, Truhlar DG, Zhang J, Kouri DJ (1986) J Phys Chem 90:6757